Snow and Ice–Symposium–Neiges et Glaces (Proceedings of the Moscow Symposium, August 1971; Actes du Colloque de Moscou, août 1971): IAHS-AISH Publ. No. 104, 1975.

Numerical modelling of glacier systems

W. F. Budd and D. Jenssen

Abstract. The aim of the project is to develop a scheme to model the dynamics of any given glacier system from the input data of bedrock distribution and accumulation or ablation (or balance) distribution as functions of time. The emphasis is on matching reality to provide a practical means of interpreting the history of change of an ice mass.

The full system of basic equations for equilibrium, ice flow properties, continuity, water production and flow are discussed in relation to theory and measurements on glaciers. A system of parameterization of the three-dimensional change of a glacier is represented by two- and one-dimensional equations. This allows a great reduction of computer time so that the complete growth and decay of an ice mass can be carried out in a reasonable time.

The numerical solution of the system of equations is described with emphasis on computational stability and problems related to iterative solutions of the velocity/stress equations.

Several particular examples of the computations carried out for given glaciers are outlined to illustrate the growth and maintenance of equilibrium. Departures from equilibrium are treated as perturbations which are found to disappear when the boundary conditions revert to equilibrium but after a pronounced phase lag.

The extension of the model to three dimensions, and the concomitant computational complexities are discussed, and future avenues of investigation indicated.

Résumé. Le but du projet est de modéliser la dynamique d'un système glaciaire quelconque en n'ayant à entrer dans le programme que la topographie du lit rocheux et la distribution de l'accumulation et de l'ablation (ou du bilan) en fonction du temps. On cherche une simulation réaliste qui donne un moyen pratique d'interpréter l'histoire des changements d'une masse de glace.

Le système complet des équations d'équilibre, de continuité, exprimant la loi de fluage de la glace, la production et l'écoulement de l'eau, est discuté à l'aide de la théorie et des mesures de terrain. Le changement tridimensionnel du glacier est représenté à l'aide d'équations à deux et à une dimensions. Cela permet une grande réduction du temps d'ordinateur, si bien que la simulation numérique complète de la croissance et la disparition d'une masse de glace peuvent être obtenues en un temps raisonnable.

La solution numérique du système d'équations est décrite, en insistant sur la stabilité des solutions et sur les problèmes relatifs à la résolution par itération des équations liant les vitesses et les contraintes.

On donne plusieurs exemples particuliers de calculs effectués pour des glaciers donnés, pour illustrer leur croissance et le maintien de leur équilibre. Les écarts à l'équilibre sont traités comme des perturbations, dont on ne constate la disparition (lorsque les conditions aux limites reviennent aux valeurs d'équilibre) qu'avec un déphasage prononcé.

On discute l'extension du modèle numérique au cas tridimensionnel, et les problèmes complexes de calcul qui en résultent; les voies de recherche futures sont indiquées.

1. INTRODUCTION

1.1 Aims and problems

The aim of the present project may be considered as two parts. First, given the dimensions of an ice mass and the flow properties of the ice, we wish to be able to calculate the velocity distribution throughout the ice mass from the equations of stress equilibrium. Second, given in addition the rate of mass exchange at the boundary (accumulation-ablation distribution), we wish to calculate from the equation of mass continuity the change of the dimensions of the ice mass with time. In attempting to solve this problem a number of serious difficulties arise. First, in order to integrate the stress equilibrium equations, we need to know the stress or velocities at the boundaries. At the surface we may take the tangential shear stress as zero and the

normal stress as atmospheric pressure. At the base the normal velocity is zero but we do not know either the tangential shear stress or velocity (sliding velocity). As a result the problem as stated is insoluble without some assumption about the base stress or velocity. However, the problem could be reframed to calculate the base stress and velocity in an ice mass given its dimensions, the flow law of ice and the velocity distribution at the surface.

A second problem is that the flow law of ice is not sufficiently well known even for 'temperate' glaciers to enable the velocity of the ice to be calculated precisely (say with less than 10% error). Glen's laboratory values of flow for ice at -1.5° and 0.02° C differed by a factor of about 4 or 5 between 1 and 2 bars. Various deductions of the flow parameters of ice from temperate glaciers, e.g. Meier (1960), Paterson and Savage (1963), Kamb and Shreve (1966) seem to lie in between the values of Glen at -0.02° and -1.5° C but the scatter is so high that to make a precise prediction of the velocity of a glacier within a factor of 2 must be considered as the best that can be expected at this stage. This all points to the urgent need for a clarification of the flow properties of ice, especially in the range of temperatures 0.00° C to -1.00° C, with precisions of temperature to 0.01° C and the effect of crystal size, shape, orientation fabrics as well as impurity and water content, all carefully controlled and varied to determine their effects on the flow rate. In addition Glen (1958) has pointed out that the influence of the stress configuration still needs further investigation. Now even if the effect on the flow law of all these parameters is known it is still a formidable problem to determine their distribution throughout the ice mass. Another approach to this problem is to determine the large scale bulk parameters that are implied from the measured velocity distributions and dimensions of ice masses. However, the difficulty of the basal boundary condition arises here too.

A third important problem is that of scale. Firstly with regard to the input data even if the surface elevation distribution of the ice mass is known it is difficult to determine the basal distribution on a horizontal scale much smaller than the ice thickness, especially if the bed topography has large irregularities. Thus any theory

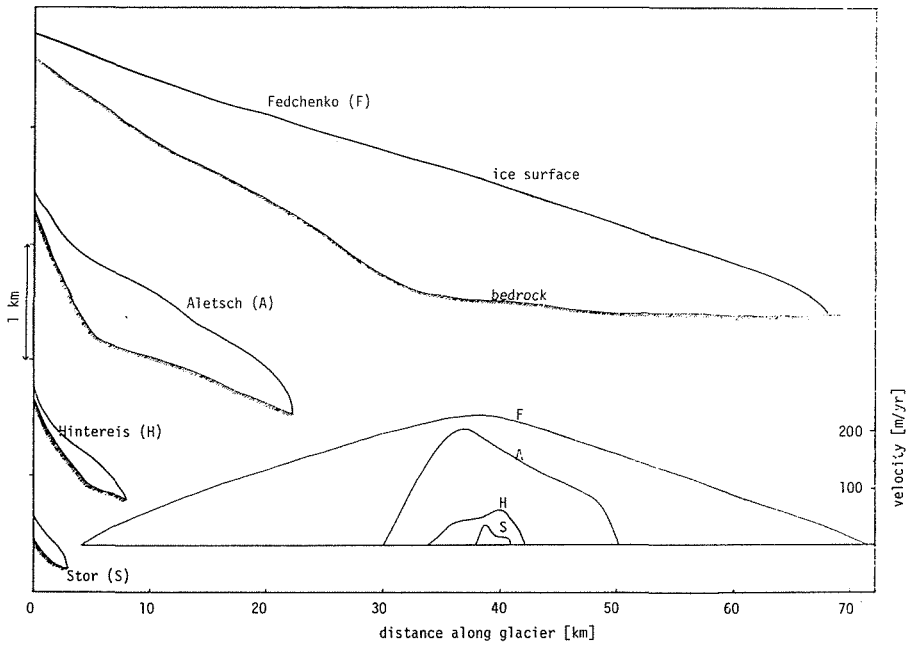

FIGURE 1. Smoothed glacier profiles and associated velocities.

which requires the knowledge of small scale irregularities will not be usable here. A further limitation on the scale resolution is the computer time required for a solution. Hence for the present study we have chosen a grid point spacing at about 2/3 of the ice thickness.

Because of these difficulties in solving the general problem we have turned to the question of how well can we calculate the velocity distribution in any given glacier from the very small (less than several kilometres) to the large (many tens of kilometres) (see Fig. 1) as well as the fast moving Greenland glaciers and the surging glaciers. Unless we can do this we can have little confidence in predicting the velocity in an existing glacier at some future or past time when its dimensions are different. The emphasis on matching reality with respect to the measurements on existing glaciers has been the main feature of the present project to date. The full project underway considers three-dimensional ice masses and through the introduction of the heat conduction equation covers cold ice masses. The present paper presents a summary of the results so far of the two-dimensional centre-line flow studies (this contains many of the important features of the dynamics of an ice mass and serves as the simplest means of comparing the model with reality), and as well indicates the direction of further work on three-dimensional calculations.

1.2 Previous glacier modelling schemes

Other methods of modelling glacier flow include that of Nye (1960, 1963a and b, 1965a and b) and Campbell and Rasmussen (1969, 1970). Nye uses the continuity equation along the line of flow (x) for the volume flux Q

$$\frac{\partial Q}{\partial x} = a(x, t) - \frac{\partial Z}{\partial t} \tag{1.1}$$

where Z is the ice thickness at distance x and time t and a is the net accumulation (balance). Here

$$Q = VZ \tag{1.2}$$

where V is the mean forward velocity.

Thus if there exists a relation between the velocity at a point and the dimensions of the ice and flow parameters at that point then equation (1.1) becomes an equation in just one unknown. Shumskiy (1965) considered that such a relation relevant to ice masses does not exist. The universal application of such a formula has not been demonstrated, but Nye (1965c and 1966) believes that it would serve as a useful starting point. He adopted for a flow relation

$$V = c_1 \alpha^n Z^{n+1} + c_2 \alpha^m Z^m \tag{1.3}$$

where α is the surface slope and c_1 and c_2 are parameters which depend on features which may be taken as constant for a given glacier such as cross-section shape, ice flow properties, bed roughness, etc., and thus vary only with x.

Here the first term on the right represents the internal deformation of the ice according to the flow law of ice. The second term represents a sliding term proportional to the mth power of the basal shear stress. This law for sliding follows Weertman's (1957) theoretical treatment. Subsequent analyses by Weertman (1962, 1964, 1969), Lliboutry (1965, 1968a and b, 1969), Nye (1969, 1970) and Kamb (1970) all aim at similar expressions in which it is considered that the sliding velocity is directly related to the basal shear stress and other properties such as the (postulated) irregularities of the bed. The existence of any such relation between velocity and basal stress is very questionable. The models used involve clearly distinct ice and rock boundaries and take no account of the direct relation between basal stress variations

and longitudinal strain rates. In addition it is apparent from studies of sliding friction of ice – Bowden and Tabor (1967), Tabor and Walker (1970) – and the low basal stress of some of the fast Greenland glaciers that the basal stress may decrease with increasing sliding velocity rather than increasing as the simple theories suppose.

Lliboutry (1968a) gives a double (and triple) valued sliding friction as a function of velocity. This still needs further experimental and field verification but can serve as a useful trial function in the meantime. Weertman (1962, 1969) also provides for a double value friction law by including the effect of the melt water film under the ice. The problem with these relations is that we do not have precise values of the parameters in them that would allow the direct application of the formulae to a numerical model.

Consequently Nye was unable to use known values in his velocity relation. To apply it in practice, Nye (1965a, b) used glaciers with measured velocity distributions which allowed the constants to be calculated. In the case of the Berendon Glacier, Untersteiner and Nye (1968) used a calculated balance velocity to determine the constants. In each case these constants were then used to follow the glacier variations in time.

The main limitation on the model is that short scale variations (wavelength $\lambda \sim 3Z$) do not follow the velocity formula involving surface slope. Budd (1969) showed that for large scales ($\lambda \sim 10Z$ or greater for temperate glaciers) the formula for velocities is approximately true but the transition scale over which the longitudinal stresses become negligible depends on the surface slope.

Secondly, without any longitudinal stress terms the model is not readily extended to treat cases where this term becomes important – such as the surges.

Campbell and Rasmussen's (1970) model made some considerable advances by extending the coverage to a complete three-dimensional system and including the effect of longitudinal stress gradients. They obtained a formula for basal stress τ_b on a medium of Newtonian viscosity ν as

$$\vec{\tau}_b = \rho g_z h \nabla h + \rho \vec{g} h + \rho \nu \nabla^2 \vec{Q} \tag{1.4}$$

where h is the surface elevation, Q is the cross-section volume flux, $\vec{g}$ is the gravitational acceleration and the vector components apply to the longitudinal and transverse directions. Then to eliminate the basal stress τ_b they introduced a linear relation between the base stress and the volume flow as:

$$\vec{\tau}_b = \frac{\vec{Q}}{A} \tag{1.5}$$

where A is a prescribed parameter.

This allowed a single equation for integrated volume flow to be obtained in terms of the dimensions and flow parameters ν and A. The partitioning of the basal stress flow parameter A from the ice viscosity allows each to be varied independently. Campbell and Rasmussen (1969, 1970) showed how this model can be used to study equilibrium profiles of glaciers, changes in time, glacier waves, glacier surges, and response times.

The agreement with real glaciers, however, will be directly related to how well the constant viscosity ν and the stress relation $\tau_b \propto Q$ apply in practice. It will be shown below that these can be easily improved upon by introducing non-linear viscosity and a relation analogous to (1.5) but agreeing with measurements on a wide range of real glaciers. The approach here has been to try to eliminate the unrealistic simplification introduced in the earlier models and to see how closely the measurements on real glaciers can be matched. The direct comparison with these other models will become apparent after section 3.

2. GENERAL PROBLEM IN THREE DIMENSIONS

2.1 Stress equilibrium

Taking orthogonal axes with x horizontal in the line of flow at the 'centre line', z vertical and y transverse the equations of stress equilibrium may be written

$$\frac{\partial \sigma_x}{\partial x} + \frac{\partial \tau_{xy}}{\partial y} + \frac{\partial \tau_{xz}}{\partial z} = \rho g_x \tag{2.1}$$

$$\frac{\partial \tau_{xy}}{\partial x} + \frac{\partial \sigma_y}{\partial y} + \frac{\partial \tau_{yz}}{\partial z} = \rho g_y \tag{2.2}$$

$$\frac{\partial \tau_{xz}}{\partial x} + \frac{\partial \tau_{yz}}{\partial y} + \frac{\partial \sigma_z}{\partial z} = \rho g_z \tag{2.3}$$

where ρ is the ice density and g_i is the gravity acceleration vector.

2.2 Boundary conditions

At the surface $z = z_1\ (x, y)$ the tangential shear stress $\tau_t)_s$ is zero and the normal stress $\sigma_n)_s$ is the atmospheric pressure p

$$z = z_1 \qquad \tau_t)_s = 0 \tag{2.4}$$

$$\tau_n)_s = p \tag{2.5}$$

At the bed $z = z_2\ (x, y)$ we have the normal velocity $v_n)_b$ zero but the tangential velocity $v_t)_b$ or tangential shear stress $\tau_t)_b$ are unknown, i.e.,

$$z = z_2 \qquad v_n)_b = 0 \tag{2.6}$$

$$v_t)_b = ? \qquad \tau_t)_b = ? \tag{2.7}$$

If we had the 'no-slip' condition at the bed $v_t)_b = 0$ and the problem would become soluble.

2.3 Flow law of ice

We adopt a generalized flow law between the second invariants of the stress deviator $\sigma'_{ij} = \sigma_{ij} - 1/3\ \delta_{ij}$ and the strain rate $\dot{\epsilon}_{ij}$ (cf. Nye, 1953, and Glen, 1958).

$$\dot{\epsilon}_{ij} = \frac{1}{2\eta}\,\sigma'_{ij} \tag{2.8}$$

where

$$\dot{\epsilon}_{ij} = \tfrac{1}{2}\left(\frac{\partial u_i}{\partial x_j} + \frac{\partial u_j}{\partial x_i}\right) \tag{2.9}$$

and where η is a generalized viscosity parameter defined by

$$\dot{\epsilon}_0 = \frac{1}{2\eta}\,\tau_0, \tag{2.8b}$$

where

$$\dot{\epsilon}_0 = (1/3\ \dot{\epsilon}_{ij}\ \dot{\epsilon}_{ij})^{\frac{1}{2}} \tag{2.10}$$

and

$$\tau_0 = (1/3\ \sigma'_{ij}\ \sigma'_{ij})^{\frac{1}{2}}$$

are the octahedral shear stress and strain rates.

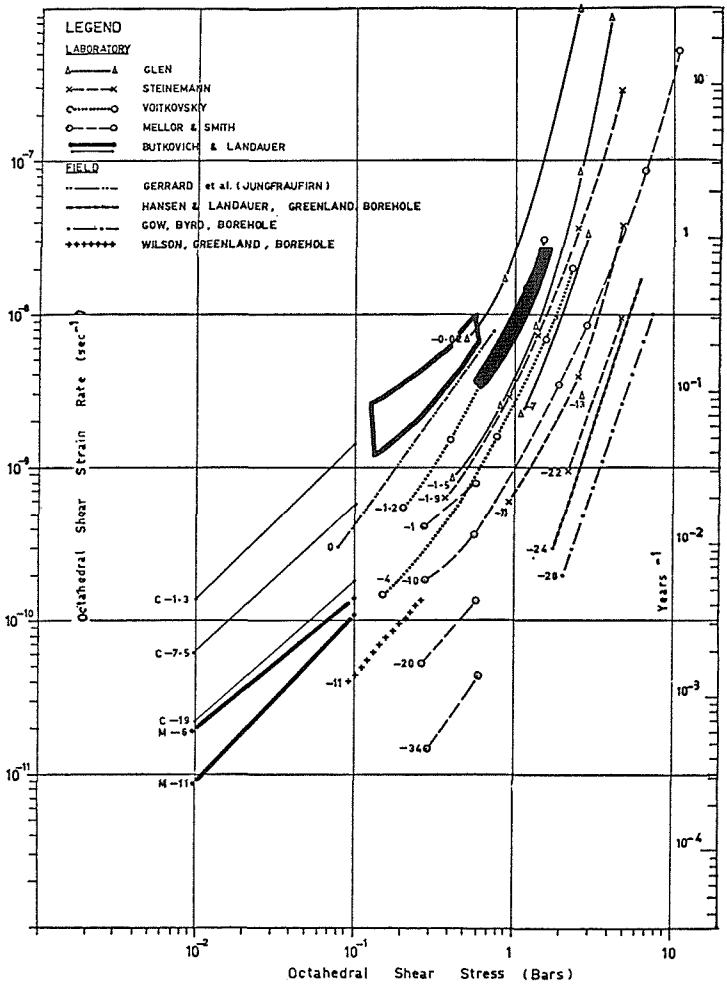

FIGURE 2. The flow law of ice. Ice strain rates versus stress from laboratory and field measurements. The values of Mellor and Smith have been extrapolated to density 0.917 g cm^{-3}. The temperatures are indicated in degrees centigrade.

The form of the relation for η is determined from measurements of the flow of ice from the laboratory and in the field (Fig. 2). The precise relation will be discussed in section 3.7. Here we note that particular forms for temperate ice may be taken as, e.g.

$$\dot{\epsilon}_0 = \frac{\tau_0}{B} \tag{2.11}$$

$$\dot{\epsilon}_0 = \left(\frac{\tau_0}{B}\right)^n \tag{2.12}$$

$$\dot{\epsilon}_0 = \frac{\tau_0}{B_1} + \left(\frac{\tau_0}{B_2}\right)^n \tag{2.13}$$

or

$$\dot{\epsilon}_0 = \epsilon_1 \sinh\left(\frac{\tau_0}{\tau_1}\right) \tag{2.14}$$

where B, n, ϵ_1, τ_1 are constants of best fit determined from the data.

2.4 Heat conduction and melting

It is apparent from the flow law of ice (Fig. 2) that since the flow parameters are temperature dependent we need to know the temperature distribution throughout the ice mass. This may be done by using the heat conduction equation (Budd *et al.*, 1971); however, this also involves the velocity distribution and so has to be solved simultaneously with the flow. For the main results of the present paper we deal only with temperate ice and assume the flow parameters are independent of temperature – in fact, we assume they vary only with stress (or strain rate). However, it must be remembered that energy dissipation in the ice could lead to difficulties such as variable water content and temperatures slightly different from the melting point depending on the impurity content (see Shumskiy, 1964; Lliboutry, 1971). These difficulties are neglected here; however the energy dissipation is largely concentrated near the bed and will cause melting which may well have an influence on the base stress and sliding velocity. If the basal shear stress is τ_b and the base velocity V_b then the energy dissipation or melt rate is given by:

$$\frac{dM}{dt} = \frac{\tau_b V_b}{JL} \tag{2.15}$$

where J is the mechanical equivalent of heat and L is the ice latent heat of fusion. Note that if a basal stress or sliding velocity can be expressed in terms of the stresses and velocities the system of equations (2.1) to (2.3), (2.4) to (2.7), (2.8) to (2.10) provide a set solvable for stress and velocity provided we have a boundary velocity (e.g. at an end point).

Once the velocity distribution is known the continuity equation can be used to determine how the ice mass changes with time.

2.5 Equation of continuity

We consider the ice as incompressible – i.e., we neglect density variations for the present. Hence we may write

$$\dot{e}_{ii} = 0 \tag{2.16}$$

Integrating over the vertical from bed to surface this becomes

$$\int_{z_1}^{z_2} \left(\frac{\partial u}{\partial x} + \frac{\partial v}{\partial y} \right) dz = w_b - w_s - \frac{\partial Z}{\partial t} \tag{2.17}$$

where u, v and w are the velocity components in the x, y and z directions and w_b and w_s are the vertical fluxes at the bed and the surface. The basal flux w_b due to melting is usually small compared with the surface flux w_s. Where necessary it may be calculated from the melt rate given by (2.15). The surface flux w_s may be replaced by the net accumulation ablation distribution, given as a function of position and time $a(x, y, z, t)$. In many cases this may simply be a function of elevation $a(z)$ or of horizontal position $a(x, y)$, only. Given this arbitrary balance function the continuity equation may be written

$$\int_{z_1}^{z_2} \left(\frac{\partial u}{\partial x} + \frac{\partial v}{\partial y} \right) dz = a - \frac{\partial Z}{\partial t} \tag{2.18}$$

Thus using the velocity distribution (u, v) from the dynamics (equations 2.8, 2.9) the equation (2.18) allows the ice thickness Z or surface elevation z_1 to be calculated as a function of time.

3. TWO-DIMENSIONAL MODEL

In order to examine the most important features of the project we consider the simplified two-dimensional model which provides a simulation of a vertical section through the central flowline of a glacier. The degree to which the two-dimensional model is useful in practice depends on the variability of the cross-section shape with distance along the line of flow. Provided the cross-section shape varies slowly along the flowline then the two-dimensional analogue is expected to provide a reasonable approximation to the actual centreline flow. The influence of the cross-section shape on the centreline flow is incorporated into the model by making use of the cross-section flow calculations of Nye (1965d), from which a system of cross-section shape factors are determined.

3.1 Cross-section flow

From the stress equations (2.1-2.3) if we consider a channel of constant cross-section shape the stress distribution across the section is governed by the equation

$$\frac{\partial \tau_{xy}}{\partial y} + \frac{\partial \tau_{xz}}{\partial z} = -\rho g \sin \alpha \tag{3.1}$$

where α is the surface slope.

Nye (1965d) solved this equation for a power law of flow to obtain velocity and stress distributions for a range of shapes for rectangles, ellipses and parabolas. He also gave an expression for the best fit shape factor s in the expression for shear stress

$$\tau_{xz} = s\rho g(\sin \alpha)z \tag{3.2}$$

i.e., for a linear variation of shear stress with depth z on the centreline for the various shapes considered.

The results of his analysis are depicted in Fig. 3 which also shows the values of the

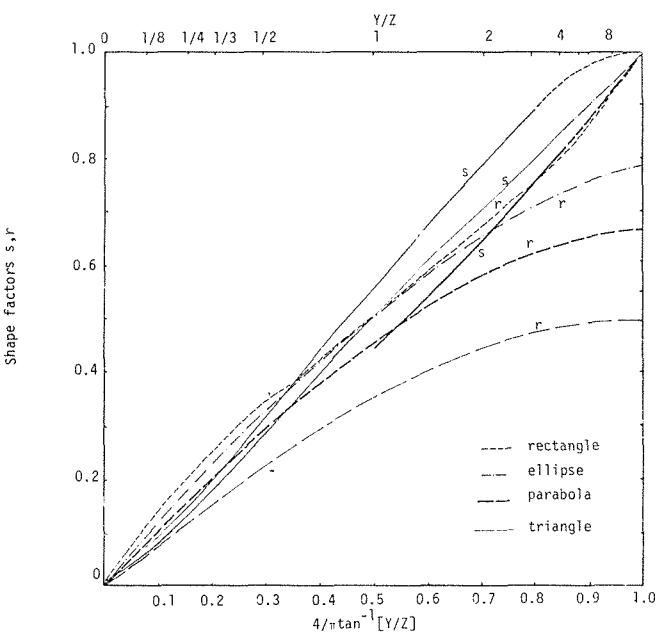

FIGURE 3. Glacier cross-section shape factors (s) and hydraulic radii (r). $s = \tau_1 / \rho g \alpha Z$ (from Nye, 1965d); $r = A/pZ$; τ_1 = central base stress; A = cross-sectional area; p = perimeter; Z = central thickness; Y = glacier $\frac{1}{2}$-width.

'hydraulic radius' shape factor

$$r = \frac{A}{pZ} \tag{3.3}$$

where A is the area of the cross-section, p is the perimeter, and Z is the thickness on the centreline.

Since the hydraulic radii tend to definite limits depending on their shapes for large widths they became much smaller than Nye's values which tend towards unity for high width to depth ratios. For the case of more complex cross-section shapes the graph of Fig. 3 may be interpolated to obtain a best fit average value. However, the more irregular and unsymmetric the shape the less applicable is this approach. If computation time were not such a serious restriction a subroutine could be incorporated to provide the cross-section calculation for the appropriate shape factor for various positions along the line. At this stage of the development the scarcity of knowledge of the ice thickness in most cases would make this unwarranted.

3.2 Two-dimensional stress system

We next consider the case of plane strain rate in two dimensions.

The stress equations may then be written

$$\frac{\partial \sigma_x}{\partial x} + \frac{\partial \tau_{xz}}{\partial z} = -\rho g_x \tag{3.4}$$

$$\frac{\partial \tau_{xz}}{\partial x} + \frac{\partial \sigma_z}{\partial z} = -\rho g_z \tag{3.5}$$

For any longitudinal direction x if z_1 is the surface and z_2 is the base, the gradient of the mean longitudinal stress deviator is given by (see Budd, 1970a)

$$-2\frac{\partial Z\bar{\sigma}'_x}{\partial x} = \rho g_x Z + Z\frac{\partial \sigma_z}{\partial x}\Big)_{z_1} - \tau_{xz_2}\tan^2\phi + \tau_{xz_1}\tan^2\theta + \frac{\tau_b}{\cos^2\phi} + \int_{z_1}^{z_2}\int_{z_1}^{z}\frac{\partial^2 \tau_{xz}}{\partial x^2}\,dz\,dz, \tag{3.6}$$

where

$$Z = z_1 - z_2, \quad \tan\theta = \frac{\partial z_1}{\partial x}, \quad \tan\phi = \frac{\partial z_2}{\partial x}$$

τ_b is the basal shear stress parallel to the bed and the subscripts z_1, z_2 represent values at the surface and bed respectively.

For small slopes of surface and bed (i.e., neglecting second orders of angles) it makes little difference whether the longitudinal axis is chosen parallel to the surface or bed or horizontal. All forms reduce to

$$2\frac{\partial(Z\bar{\sigma}'_x)}{\partial x} = \rho g Z\alpha - \tau_b - \int\int\frac{\partial^2 \tau_{xz}}{\partial x^2}\,dz\,dz \tag{3.7}$$

where α is now the downward slope of the surface with respect to the horizontal in the direction of flow.

3.3 Scales of variation

The terms in equation (3.7) have different relevance over three different scales. It was shown by Budd (1970b, 1971) that for short wavelength variations, $\lambda < 2\pi Z$, the last

term

$$T = \int\int \frac{\partial^2 \tau_{xz}}{\partial x^2}\, dz\, dz \tag{3.8}$$

becomes important. For long waves, however, say $\lambda > 10Z$, this term becomes small.

Over the whole length of the glacier if the ends go to zero thickness or are free then the equation for the mean basal stress $\bar{\tau}_b$ over the length is given by

$$\bar{\tau}_b = \rho g \int_0^X \alpha Z\, dx$$

$$= \rho g \alpha \bar{Z} \tag{3.9}$$

Since the average of the longitudinal stress deviator gradient, namely

$$\frac{1}{x_2 - x_1} \int_{x_1}^{x_2} G\, dx = \frac{1}{x_2 - x_1} \int_{x_1}^{x_2} \frac{\partial Z\bar{\sigma}'_x}{\partial x}\, dx = \frac{Z\bar{\sigma}'_x)_{x_2} - Z\bar{\sigma}'_x)_{x_1}}{x_2 - x_1} \tag{3.10}$$

usually decreases with increasing averaging distance $(x_2 - x_1)$, the relation for $\bar{\tau}_b$, equation (3.9), holds closely provided $(x_2 - x_1)$ is large enough.

Thus we define the terms: 'small scale', where the term T is important; 'large scale', where $\tau_b \simeq \rho g \alpha \bar{Z}$; 'intermediate scale', where the term G is important but T is not. The relative magnitude of these various terms for harmonic variations along the flowline has been discussed by Budd (1969, 1970b and 1971).

For the present we shall consider only the intermediate and large scales i.e., neglecting T. For small scale or short wavelength variations T must be included and this can be achieved by considering perturbations superimposed on the smoothed values.

3.4 Basic longitudinal stress equation

Thus we examine the equation

$$2 \frac{\partial Z\bar{\sigma}'_x}{\partial x} = \rho g \alpha Z - \tau_b \tag{3.11}$$

For a smooth slab with small slope and on a rough bed the three terms in equation (3.11) represent respectively the net force across the ends $2G$, the down slope gravity force $\rho g \alpha Z$ and the base stress τ_b, upslope. The base stress causes vertical shear in the ice and we may use this to express τ_b in terms of the ice deformation.

Using the shape factor introduced in section (3.1) the shear stress τ_{xz} at depth z may be written $\tau_{xz} = s\rho g \alpha z$. Thus the two-dimensional stress equation (3.11) can be used for the centreline flow in the form

$$2 \frac{\partial Z\bar{\sigma}'_x}{\partial x} = s\rho g \alpha Z - \tau_b \tag{3.12}$$

3.5 Basal shear stress in terms of deformation

Now if we use a power flow law of the type (2.12) and assume for the moment that the horizontal shear stress is much larger then other stress deviators here, the velocity gradient in the vertical becomes

$$\frac{1}{2} \frac{du}{dz} = \left(\frac{s\rho g \alpha z}{B} \right)^n \tag{3.13}$$

Hence

$$u_s - u_b = \frac{2}{n+1}\left(\frac{s\rho g \alpha Z}{B}\right)^n Z$$
$$= \frac{2}{n+1}\left(\frac{\tau_b}{B}\right)^n Z \tag{3.14}$$

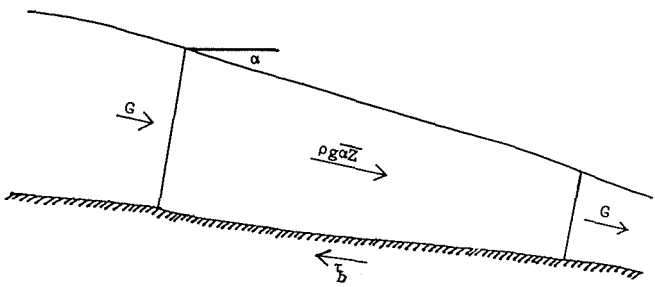

FIGURE 4. Net forces on a longitudinal section.

From this we find for the base stress

$$\tau_b = B\left[\frac{n+1}{2}\,\frac{u_s - u_b}{Z}\right]^{1/n} \tag{3.15}$$

If we assume that even in the presence of a longitudinal stress gradient this expression still holds for the base stress we may substitute it in equation (3.12) to yield

$$2\,\frac{\partial Z\overline{\sigma'_x}}{\partial x} = s\rho g \alpha Z - B\left[\frac{n+1}{2}\,\frac{u_s - u_b}{Z}\right]^{1/n} \tag{3.16}$$

which is now an equation for longitudinal stress in terms of an unknown basal sliding velocity u_b instead of an unknown base stress τ_b.

3.6 Longitudinal stress in terms of velocity

The longitudinal stress gradient may be converted to longitudinal strain rate by use of a flow relation, e.g.:

$$\overline{\sigma'_x} = 2\overline{\eta\dot{\epsilon}_x} \tag{3.17}$$

Substituting in (3.16) gives

$$4\,\frac{\partial Z\overline{\eta\dot{\epsilon}_x}}{\partial x} = s\rho g \alpha Z - B\left[\frac{n+1}{2}\,\frac{u_s - u_b}{Z}\right]^{1/n} \tag{3.18}$$

At this stage we make the further assumption that

$$\overline{\eta\dot{\epsilon}_x} = \bar{\eta}\,\bar{\dot{\epsilon}}_x$$

where $\bar{\dot{\epsilon}}_x$ is the mean velocity gradient through the thickness which is the same as the gradient of mean velocity. This in effect defines the average flow parameter $\bar{\eta} = \overline{\eta\dot{\epsilon}_x}/\bar{\dot{\epsilon}}_x$.

The mean downslope velocity is given by

$$V = \frac{1}{Z}\int_0^Z u_z\, dz = u_b + \frac{n+1}{n+2}(u_s - u_b)$$
$$= \frac{n+1}{n+2}u_s + \frac{1}{n+2}u_b \tag{3.19}$$

Equation (3.18) may now be written in terms of mean velocity as

$$4\frac{\partial \bar{Z\eta}\frac{\partial V}{\partial x}}{\partial x} = s\rho g\alpha Z - B\left[\frac{n+2}{2}\frac{V-u_b}{Z}\right]^{1/n} \tag{3.20}$$

The corresponding relation in terms of the surface velocity is

$$4\frac{\partial}{\partial x}\left\{\frac{\bar{Z\eta}}{n+2}\left[n+1\frac{\partial u_s}{\partial x}+\frac{\partial u_b}{\partial x}\right]\right\} = s\rho g\alpha Z - B\left[\frac{n+1}{2}\frac{u_s-u_b}{Z}\right]^{1/n} \tag{3.21}$$

This means that given the dimensions (α, Z) and the flow parameters ($\bar{\eta}$, n, B) together with the surface velocity distribution, the basal sliding velocity is determined. Since errors in the flow parameters and the glacier dimensions can lead to considerable errors in the various terms, then unless both the dimensions and flow parameters are known precisely this equation cannot, at this stage, be used practically to determine the sliding velocity.

3.7 Values of flow parameters – velocities and dimensions of glaciers

Since we are here interested in knowing the flow parameters which when substituted into equations such as (3.20) or (3.21) together with the glacier dimensions give the correct velocity distribution we now examine the results of measured velocities on glaciers to see what may be determined about the sliding velocities.

Over large horizontal scales the term

$$\frac{1}{x_2-x_1}\int_{x_1}^{x_2}\frac{\partial \bar{Z\sigma'_x}}{\partial x}\,dx$$

is generally small except near irregularities such as ice falls. Hence the available data were examined for glaciers with measured surface velocity, surface slope, ice thickness and width and where possible cross-section shape, in regions of small longitudinal strain rate. Large scale values were taken where possible i.e., surface slope and ice thickness α,Z were taken with averages of $\bar{\alpha Z}$ over about 10 times the ice thickness. This resulted in a great deal of spurious irregularity being eliminated and the final character of the variations of velocity along a glacier as well as that from one glacier to another became comparatively systematic.

Although a large number of measurements of individual velocities, ice thickness and slopes are available only a small proportion of these have all the data. Even so some 57 glaciers have been examined including 22 rapidly moving Greenland glaciers but excluding clearly cold glaciers here. The complete details of the analysis of these data will be given elsewhere. Here we turn to just two results of this analysis. The first is illustrated by Fig. 5 which shows the plot of surface velocity at the centre against the central base stress as calculated from

$$\tau_c = s\rho g\bar{\alpha Z} \tag{3.22}$$

The fast Greenland glaciers, which are omitted here, form a distinct group about one or two orders of magnitude greater in velocity over the same stress range. The stresses range from about 0.5 bar to 2 bars and for each stress the velocities have a range of magnitudes of about an order of magnitude which appear to be strongly dependent on the ice thickness.

From the relation (3.14)

$$u_s - u_b = \frac{2}{n+1}\left(\frac{\tau_b}{B}\right)^n Z$$

the differential motion for a constant stress is directly proportional to the ice thickness. This effect is removed by dividing by the ice thickness.

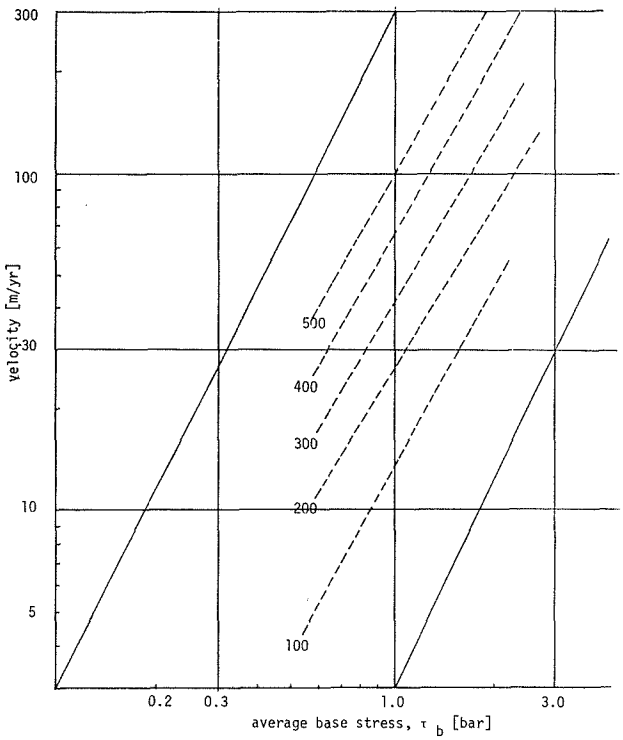

FIGURE 5. Velocity versus base stress. $\tau_b = s\rho g\alpha Z$. Dotted lines are contours of ice thickness in metres, contour values are given by the numbers.

Hence we examine the relation

$$\frac{u_s}{Z} = \frac{2}{n+1}\left(\frac{\tau_b}{B}\right)^n + \frac{u_b}{Z} \tag{3.23}$$

For a power flow law of the form

$$\dot{\epsilon}_{xz} = \left(\frac{\tau_{xz}}{B}\right)^n$$

the strain rate at the bed is given by

$$\dot{\epsilon}_{xz})_b = \frac{1}{2}\left(\frac{\partial u}{\partial z}\right)_b = \left(\frac{s\rho g\alpha Z}{B}\right)^n \tag{3.24}$$

Hence

$$\frac{1}{2}\left(\frac{\partial u}{\partial z}\right)_b = \frac{n+1}{2}\left(\frac{u_s - u_b}{Z}\right) \tag{3.25}$$

Thus the plot of

$$\frac{n+1}{2}\,\frac{u_s}{Z}$$

against τ_b should lie above the flow law curve

$$\dot{\epsilon}_{xz} = \left(\frac{\tau_{xz}}{B}\right)^n$$

by an amount due to the sliding

$$\left(\frac{n+1}{2}\right)\frac{u_b}{Z}$$

Figure 6 shows the plot of u_s/Z against $\bar{\tau}_c$. The range of scatter of a factor of 10 in u_s from Fig. 5 is reduced to less than 50% in u_s/Z for the ordinary glaciers whose velocity is less than 300 m/yr. The fast moving Greenland glaciers form their own group one to two orders of magnitude higher in u_s/Z over much the same $\bar{\tau}_c$ range, viz. 0.5 to 2.0 bars. This range of stress is quite small but it accounts for a clear order of magnitude increase in u_s/Z. Many of the glaciers considered showed considerable annual variation in surface velocity suggesting that sliding may account for an appreciable part of the annual mean velocity. In order to see the amount of expected differential motion we superimpose the data here on the diagram of measurements of the flow of ice. All values are shown converted to octahedral values of shear strain rate and stress in Fig. 2.

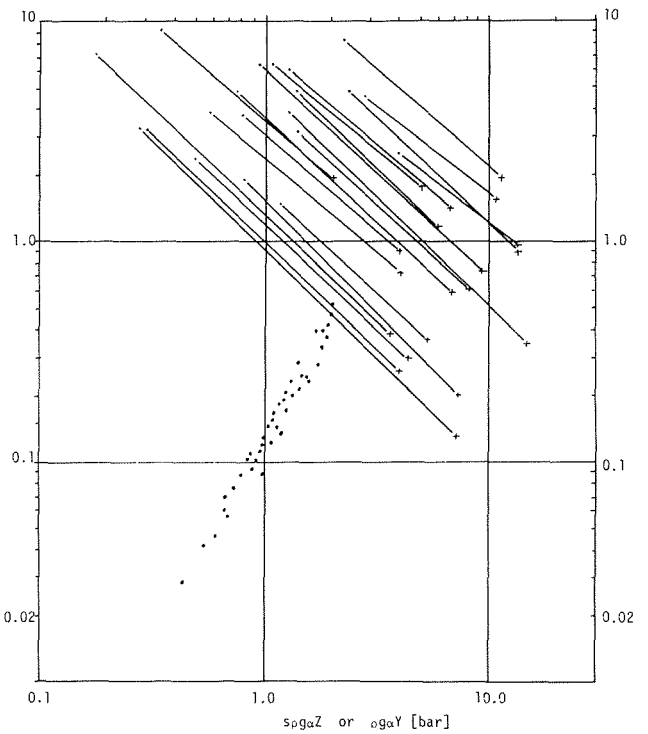

FIGURE 6. Mean strain rate versus base stress. Dots give the relation between u_s/Z (where u_s is the surface velocity, Z is the ice thickness) [year^{-1}] and the base stress. Further details are found in the text.

The present data lie between the values of Glen's measurements (1955) at -0.02°C and -1.5°C. In the calculations from the data, errors of only 5% in the velocity V, ice thickness Z, surface slope α, and shape factor s could easily amount to 30% in the plot of u_s/Z versus $s\rho g\alpha Z$. This suggests that although sliding may be an appreciable part of the total movement it is easily masked by errors in the data. A systematic error may be introduced by the shape factor from Fig. 3 being generally too high as indicated by the difference between Nye's (1965d) values and the hydraulic radii. The maximum error

from this would result in about a 10% lowering of stress for the points in Figs. 6 and 2. Results from some borehole measurements also give similar strain rates but it must be remembered that boreholes are essentially very local and may suffer from high variability especially near the bed.

By contrast to the ordinary or main sequence of glaciers the fast moving Greenland glaciers are apparently sliding over their beds at the centre, but may be fixed at their sides. The details of the mechanics of this process are governed by essentially three-dimensional features and will be given elsewhere.

Here we merely state that for the ordinary glaciers we may expect to be able to calculate the large scale average velocity distribution from the data curve of Fig. 6 together with the dimensions assuming deformation only with no slip. For high velocities there is apparently major sliding setting in, which appears to involve at least a double valued relation for velocity against base stress. The model we have developed aims at including this effect, allowing it to treat such problems as surging glaciers which appear to pass from one state to the other. This aspect will be treated fully elsewhere. For the moment we follow the no slip model.

From the data curve of Fig. 6 we adopt the relation

$$\frac{V}{Z} = k\tau_b{}^n \tag{3.26}$$

where V is the mean forward velocity and $n = 2.5$ and

$$k = \frac{n+1}{n+2}\ 0.11\ \text{yr}^{-1}\ \text{bar}^{-n}$$

For the longitudinal stress rate, however, we need to cover a much greater range of stress so we use the relation

$$\dot{\epsilon}_x = E_0\ \sinh\left(\frac{\tau}{\tau_1}\right) \tag{3.27}$$

where $E_0 = 0.685\ \text{yr}^{-1}$ and $\tau_1 = 0.3$ bar.

This also fits the above flow law data quite closely as well as the shape of the other data curves for higher and lower stresses.

3.8 Calculation scheme for velocity

The routine of the calculation of velocity and base stress can be given as:

(1) For the base stress take:

$$\tau_b = s\rho g\overline{\alpha Z} - 2\frac{\partial}{\partial x}\left[Z\tau_0\ \underset{\tau_0\to\tau_1}{\sinh^{-1}}\left(\frac{\partial V}{\partial x}\Big/E_0\right)\right] \tag{3.28}$$

where αZ is smoothed over about 10 times the ice thickness.

(2) The velocity (smoothed) is:

$$\frac{V}{Z} = k\bar{\tau}_b{}^n \tag{3.29}$$

(3) This is substituted into (3.28) to give the expression:

$$\left(\frac{V}{\overline{Zk}}\right)^{1/n} = s\rho g\bar{\alpha}\bar{Z} - 2\frac{\partial\left[Z\tau_0\ \underset{\tau_0\to\tau_1}{\sinh^{-1}}\left(\frac{\partial V}{\partial x}\Big/E_0\right)\right]}{\partial x} \tag{3.30}$$

the solution of which will give the velocity distribution. The details are given in section 4. The form of the equation corresponds to that of Campbell and Rasmussen (1970). It is expected that their results would give a better approximation to reality for the ordinary glaciers by using

$$Q = k\tau_b{}^n Z^2 \quad \text{with} \quad n \sim 2$$

and by making ν a non-linear parameter and keeping it inside the second derivative of the ∇^2 term.

The smaller scale variations may be considered as perturbations from this smoothed profile from the theory of Budd (1970b, 1971). In the case of medium scale waves the base stress fluctuations τ'_b and the longitudinal stress rate deviations

$$G' = \left(\frac{\partial Z\eta\dot{\epsilon}_x}{\partial x}\right)'$$

are both proportional to the fluctuations in the surface slope α'

$$G' \simeq \tau_b{}' \simeq s\rho g\alpha' Z \tag{3.31}$$

For short wave fluctuations it is necessary to know the wavelengths, thus a harmonic or spectral representation of the surface and the bed are required.

3.9 Continuity and time change

Having determined the velocity the continuity equation is then used to determine the change with time. For the two-dimensional model the continuity equations may be taken as:

$$\frac{\partial \bar{Y}\bar{V}Z}{\partial x} = \bar{a}Y - Y\frac{\partial Z}{\partial t} \tag{3.32}$$

where Z is the centreline thickness at x, $\bar{Y}$ is the mean cross-section width, $\bar{V}$ is the mean velocity across the section, $\bar{a}$ is the mean accumulation rate across the section, Y is the surface width.

We define a second shape factor by:

$$\bar{Y}\bar{V} = s_2 YV \tag{3.33}$$

Then the continuity equation takes the form:

$$\frac{\partial s_2 YVZ}{\partial x} = \bar{a}Y - Y\frac{\partial Z}{\partial t} \tag{3.34}$$

The width Y, accumulation rate a and shape factor s_2 which is calculated from Nye's (1965a) results for cross-section flow, are normally fed in as input data at the commencement and kept constant. However, it is also possible to prescribe them as a function of ice thickness Z (or elevation) as well as x so that they vary realistically as the ice mass grows or decays.

In addition if the accumulation rate, a, is specified as a function of time as well, then the continuity equation will follow the reaction of the glacier to this.

The steady state ice mass shape for an accumulation profile constant with time, is obtained by simply letting the glacier grow until the rate of change is sufficiently close to zero (e.g., less than 1 cm/century).

4. COMPUTER SOLUTION

4.1 Application of the problem to a computer

In order to apply the model discussed in section 3 to a computer some preliminary analysis of the governing equations and selection of data must be made. The model

depends essentially on equations which allow the velocity distribution to be found, and the change in ice thickness to be deduced from the existing thickness and the just-computed velocities. To use these equations some approximations must be made, and the range over which these equations are valid must be found. Section 4.2 below discusses iterative means of finding the velocity, and section 4.3 treats the integration of the continuity equation in time. In both cases it is found that unless certain inequalities are satisfied the resulting computations are valueless.

Even after the convergence and stability criteria are satisfied, however, problems can arise due to the accumulation of errors involved in using a finite number of significant figures in the computation. This is the topic of section 4.4. Further problems arise in boundary conditions, particularly at the snout of the glacier; section 4.5 covers these.

As is customary, the exact derivatives in the relevant equations must be replaced by finite differences, of which there are many available (vide Jenssen and Straede, 1969). In order to do this some set of discrete points must be chosen along the glacier, and data at only those points used. This will be discussed in section 4.6, but it must be pointed out here that the model is one-dimensional inasmuch as all parameters (accumulation, bedrock elevation, and so forth) are functions of one space variable only.

4.2 The determination of the velocity distribution

The equations governing the flow of the glacier have already been given in section 3 and as far as the computational model is concerned, they are written in the combined form of equation (3.30):

$$\left(\frac{V}{kZ}\right)^{1/n} + \rho g \bar{\alpha} s Z - 2\tau_0 \frac{\partial}{\partial x}\left(Z \sinh^{-1}\left[\frac{1}{E_0}\frac{\partial V}{\partial x}\right]\right) = 0 \qquad (4.1)$$

The method of solution is a straightforward iterative scheme, wherein a guess to the velocity is successively corrected, the process being represented by:

$$V^{\nu+1} = V^{\nu} + rR^{\nu} \qquad (4.2)$$

where ν denotes the iteration number (*not* an exponent), R is the value of the L.H.S. of (4.1) when V^{ν} is substituted in it for V, and r is some quantity on which the rate of convergence depends. The following analysis determines the analytic form of r.

Assume that the speed at any iteration is given by the true value V^*, and an error ϵ,

$$V^{\nu} = V^* + \epsilon^{\nu} \qquad (4.3)$$

If it is noted that $\sinh^{-1}(x + x') < x' + x$ when $x' \ll x$, and x is any dimensionless number, then use of (4.3) will lead to the linearized form of the equation (4.1):

$$\frac{\tau^*}{nV^*}\epsilon^{\nu} - 2\tau_0 \frac{\partial}{\partial x}\left(\frac{Z}{E_0}\frac{\partial \epsilon^{\nu}}{\partial x}\right) = R^{\nu}$$

It has been assumed here, of course, that ϵ is very small compared with V. If, now, the error ϵ is expressed as a Fourier series

$$\epsilon^{\nu} = \sum_{i=1}^{p-1} A_p^{\nu} \sin(\pi p i/P) \qquad (p = 1, 2, 3 \ldots P-1)$$

then the linearized (4.1) becomes (if only one component of the series is considered for the moment):

$$R^{\nu} = \epsilon^{\nu}\left[\frac{\tau^*}{nV^*} - \frac{2\tau_0}{E_0\,\Delta x}\,\frac{\partial Z}{\partial x}\,\frac{\sin \pi p/P}{\tan \pi pi/P} + \frac{8\tau_0 Z}{E_0\,\Delta x^2}\sin^2 \pi p/2P\right] = W\epsilon^{\nu} \qquad (4.4)$$

Here, Δx results from the approximation

$$\frac{\partial \epsilon}{\partial x} \simeq (\epsilon_{p+1} - \epsilon_{p-1})/2\Delta x$$

Using (4.2), the above shows that:

$$\epsilon^{\nu+1}/\epsilon^{\nu} = 1 + rW$$

Clearly for the iterative scheme to converge it is necessary that $|\epsilon^{\nu+1}/\epsilon^{\nu}| < 1$. Since W depends upon the error distribution, the high and low frequency errors will, in general, have different convergence rates. To overcome this deficiency, and in fact to ensure that they have the same convergence rate it is required that:

$$|1 + rW_{\max}| = |1 + rW_{\min}|$$

From the definition of W given above, it is noted that $W_{\max}$ will occur when $\tan(\pi pi/P) < 0$ and $\sin^2 \pi p/2P$ has its maximum value. Thus:

$$r = -\left[\frac{\tau^*}{nV^*} + \frac{8\tau_0 Z}{E_0\,\Delta x^2}\{(\sin^2 \pi p/2P)_{\max} + (\sin^2 \pi p/2P)_{\min}\}\right]^{-1}$$

or, making some approximations,

$$r = -\left[\frac{\tau^*}{nV^*} + \frac{8\tau_0 Z}{E_0\,\Delta x^2}\right]^{-1} \qquad (4.5)$$

This gives an optimum (or best) value for the relaxation constant, but does not indicate whether or not this convergence will actually occur. The convergence rate, however (which is the same now for both high and low frequencies), is given by:

$$\left|\frac{\epsilon^{\nu+1}}{\epsilon^{\nu}}\right| = \left\{\frac{2\tau_0 L}{E_0\,\pi\Delta x^2}\left|\frac{\partial Z}{\partial x}\right|\right\} \Big/ \left\{\frac{\tau^*}{nV^*} + \frac{8\tau_0 Z}{E_0\,\Delta x^2}\right\} \qquad (4.6)$$

and it can be seen that only when:

$$\left|\frac{\partial Z}{\partial x}\right| < \frac{4\pi Z}{L} + \frac{E_0\,\pi\tau^*\,\Delta x^2}{2n\,\tau_0 V^* L}$$

will the solution converge. This criterion depends on the grid spacing Δx used to represent the glacier as a series of points, and the smaller that spacing becomes, the less rapidly can the depth vary with distance. In the limit

$$\left|\frac{\partial Z}{\partial x}\right| < \frac{13.5Z}{L}$$

and provided this is satisfied, any arbitrary grid spacing may be used. Generally, (4.6) will be satisfied, but should some case arise where it is violated then other iterative techniques may be employed, and one will be briefly indicated later.

Returning to equation (4.5) an interesting point emerges, namely that the optimum value of the relaxation constant depends on the solution itself. Since this is not known – indeed the whole point is to find it – the values for $V^*\,\tau^*$ must be estimated by some other means; this is simply accomplished by assuming that $V^* = V^{\nu}$ in (4.5).

To speed up the convergence somewhat, an accelerated scheme is employed, in which the $V^{\nu+1}$ are replaced in the grid as they are formed. Although this will change the value of the constant r, it is assumed that it will be a slight variation only. Calculations have been made for the procedure described above, and for the accelerated scheme, in both of which r is given by (4.5), and it was found that the accelerated method was in fact faster. The iterative process is extremely powerful (probably due to the fact that the relaxation constant changes with position in the grid and with the iteration number) and generally only some four or five passes are required to reduce all the R^{ν} by about a factor of 10^{13}. The corresponding error in speed is then never greater than 1%. Strictly speaking, of course, the quantity r should not be termed a constant – it has been done so here in accordance with the terminology of relaxation schemes.

It was mentioned above that other iterative schemes may be developed. Very briefly, one method is to take the second and third terms of (4.1) to the right hand side and to substitute V^{ν} for V in them, but to replace V by $V^{\nu+1}$ in the first term, thereby allowing the new iterative value to be found. If the convergence rate is determined in this case by means analogous to those just given, it is found that the criterion (4.6) holds, but with an important change: the left hand side of the inequality is no longer in the modulus brackets. That is, the depth decrease with distance need no longer be bounded for convergence. Since it has been found that (4.6) is most likely to be violated toward the snout of a glacier, it is probable that the alternative iterative scheme will be of greater applicability since it can handle rapidly thinning glaciers. Unfortunately, the drawback to this method is the very much longer time needed for convergence. No relaxation constant at all is involved here, and the procedure is of necessity slow. Nonetheless, it provides a valid alternative should one become necessary.

It is interesting to investigate the effects of violating (4.6) by arbitrarily making r too large. When this is done, and r is not too big, convergence apparently results in that the errors decrease rapidly. If, however, the iterations continue, there comes a time (after say 25 iterations) when the errors again amplify, and divergence very quickly results. This means that in the course of the computations, although for the first few time steps the process may appear convergent, the true divergent nature of the iterative scheme eventually will cause totally invalid results to ensue. These errors will manifest themselves as though computational instability was their cause. It is therefore very important to ensure that (4.6) is always satisfied, since experimentation has shown it to be an extremely sensitive inequality.

4.3 Computational stability

The integration of the continuity equation for constant width and unit shape factor s_2 is (see equation 3.34):

$$\frac{\partial Z}{\partial t} = \bar{a} - \frac{\partial}{\partial x}(ZV) \tag{4.7}$$

In time this requires that the time step employed (Δt) and the grid interval (Δx) satisfy another inequality. If this is not done then any small errors present in the data, or due to machine round-off, will amplify and eventually swamp the true solutions. A crude method of estimating the stability criterion is given below.

Assuming that $V \simeq k(-\rho g s \bar{\alpha})^n Z^{n+1}$ and that

$$\alpha = \frac{\partial B}{\partial x} + \frac{\partial Z}{\partial x}$$

where B is now the bedrock elevation, (4.7) becomes

$$\frac{\partial Z}{\partial t} = \bar{a} - \frac{\partial}{\partial x}\left[k(-\rho g s)^n \left(\frac{\partial B}{\partial x} + \frac{\partial Z}{\partial x}\right)^n Z^{n+2}\right]$$

Following the previous section the depth is written as $Z = Z^* + d$, where d is the error at the current time. It follows that if $\bar{\alpha} = \alpha^* + \alpha'$,

$$\frac{\partial d}{\partial t} = -d(n+2)\frac{\partial V^*}{\partial x} - \left[(n+2)V^* + n\frac{\partial}{\partial x}\left(\frac{V^* Z^*}{\alpha^*}\right)\right]\frac{\partial d}{\partial x} - n\frac{V^* Z^*}{\alpha^*}\frac{\partial^2 d}{\partial x^2}$$

By further assuming that $d = g(t)f(x)$ (that is, that the error is a product of a function of time and a function of space), that $f(x) = \Sigma A_q \sin(\pi qj/Q)$ $(q = 1, 2, 3, \ldots Q-1)$, and that forward difference analogues are used for the time derivative and centred ones for the space derivative, the equation above is transformed to:

$$\frac{g(t+\Delta t)}{g(t)} = 1 - \Delta t\left[-(n+2)\frac{\partial V^*}{\partial x} - \frac{1}{\Delta x}\left\{(n+2)V^* + n\frac{\partial}{\partial x}\left(\frac{V^* Z^*}{\alpha^*}\right)\right\}\frac{\sin \pi q/Q}{\tan \pi jq/Q} + \frac{4n\, V^* Z^*}{\alpha^* \Delta x^2}\sin^2 \pi q/2Q\right] \qquad (4.8)$$

$$= 1 + U\Delta t$$

If any errors, which are always present, are not to grow with time, it is clear that $|g(t + \Delta t)/g(t)| < 1$, which in turn requires that

(a) $U < 0$

and

(b) $|U|_{\max} \Delta t < 2$

or

$$\Delta t < 2/|U|_{\max}$$

Assuming, for the moment, that (a) is satisfied, then criterion (b) demands that

$$\Delta t < \frac{2\Delta x^2}{\dfrac{4V^* Z^*}{|\alpha^*|} + \Delta x^2 (n+2)\left|\dfrac{\partial V^*}{\partial x}\right|_{\max} + \dfrac{L}{\pi}\left[n\dfrac{\partial}{\partial x}\left(\dfrac{V^* Z^*}{\alpha^*}\right) + (n+2)V^*\right]_{\max}} \qquad (4.9)$$

This is a complex inequality to evaluate, but rough calculations on a few realistic glaciers suggest that the first term is the dominant one – which, as will be seen in a moment, it must be if criterion (a) is to be satisfied – and that, very crudely,

$$\Delta t < \frac{\Delta x^2 \, |\alpha^*|}{2V^* Z^* n} \qquad (4.10)$$

Reverting back to equation (4.8), it can be seen that only the term on the right hand side which is dependent on sine^2 has the same sign always, and therefore that the stability of the integration procedure is determined by its relative magnitude in comparison with the other terms. In fact it must be larger than the sum of the other

two terms in the square brackets, and as well be negative in order to ensure that U is less than zero. This in turn implies that the surface slope, α, must always be negative; that is, that the glacier always has a downslope. From this it follows that if criterion (a) is to be fulfilled, then the approximation made to reach (4.10) is also valid, and conversely if that criterion is met, then (a) will be also.

The restriction that the surface slope shall be always negative is perhaps too stringent, and may be relaxed in some cases without instability resulting. For example, if the upslope is not fixed with time to a particular point of the glacier, or it is not too large, or does not persist for too long a time. In other words, momentary, moving upslopes are permissible – a conclusion substantiated by experimental calculations.

It is now possible to sum up the computational procedure in broad outline; other details are given in section 4.6. First, from the initial data supplied to the computer the velocity distribution is determined by solving (4.1) by iterative means; secondly, these new velocities are used in equation (4.7) to find the new depths through

$$Z^{t+\Delta t} = Z^t + \Delta t\left[\bar{a} - \frac{\partial}{\partial x}(ZV)\right] \tag{4.11}$$

subject to the stability criterion (4.10). The programme then cycles back to the first step and continues until the desired time has been reached, or the computation becomes uninteresting.

4.4 Smoothing

The mere fact that any computer is limited in the number of significant places it can carry means that round-off errors must occur. Normally these are not important, but when, as is the case here, many time steps are involved in the integrations they can accumulate and grow.

They thus represent a source of very high frequency errors, and even if criterion (4.10) is satisfied, instability can result. (This is a common finding in, for example, numerical weather forecasting.) These short wavelength errors, superimposed on the basic error field due to unsmooth data or observational error, must be eliminated, or at best kept to a minimum. To do this the data are smoothed at certain times during the integration. These times may be preset (after say every 200 time steps), arbitrarily determined by man/machine interaction, or performed by the programme on the onset of large amplitude high frequency errors. It is the last scheme which is usually used, though provision exists in the programme for the others.

At every time step the velocity distribution is scanned and if any five successive points exhibit a rise-and-fall behaviour between all contiguous points, and the amplitude of this fluctuation is greater than a tenth of the velocity at the relevant point, smoothing is effected. (Thus, for example, the following set of velocities will lead to smoothing:: . . . 100, 120, 98, 118, 102, . . . etc.)

Smoothing is very simple, and is merely

$$V \leftarrow V + \frac{1}{4}\frac{\partial^2 V}{\partial x^2} \tag{4.12}$$

where the arrow means 'is replaced by'. It is velocity which is the field chosen for smoothing since experimentation has shown that computational instability which results from round-off is manifest earliest and most clearly there.

Smoothing of the data will also eliminate some features which may be real and not due to computational techniques; however, it is thought that since smoothing occurs only when absolutely necessary very little of the important structure of the basic fields will be lost.

4.5 Boundary problems

There are very few boundary conditions which need to be specified or met in the model. Such features as accumulation, bedrock elevation, initial ice thickness, shape factors and so on present no difficulties, and their specification is discussed in the section following. Boundary conditions for the velocity – at the source and snout of the glacier – are somewhat tricky.

It is assumed that the velocity at the source is always zero; that is, either the bedrock slopes upward so sharply as to constitute a wall there, or the source is placed at the highest elevation of a glacier which has non-zero depth there, and this point is therefore singular. For the snout the velocity is generally indeterminate since the exact end of the glacier will coincide very seldom with a point of the fixed grid which lies along the length of the ice mass. Two schemes have been tried. The first results directly from equation (4.1): as the ice thickness approaches zero, so also will the base stress and hence so must the velocity. Thus at the snout, velocity is set to zero. The second assumes that whenever the ice thickness is less than some arbitrary amount (say 50 m) the snout moves forward as a block. It has been found experimentally that there is little difference between these two methods, and since the former at least has the virtue of being consistent with the basic equation for velocities, it is used.

It has been noted that the ice flows past the grid, and that the extreme end of the snout is 'lost sight of'. Additional computations are therefore necessary to track it. If the glacier lies a distance b^t away from the last grid point at some time t, and if it is assumed that the snout has a triangular shape, then the mass of the snout at time $t + \Delta t$ is given by the sum of the old mass, the accumulated (or ablated) ice, and the mass flow past the last grid point. That is:

$$\frac{1}{2} b^{t+\Delta t} Z_n^{t+\Delta t} = \frac{1}{2} b^t Z_n^t + \Delta t V_n^t (Z_n^t + Z_n^{t+\Delta t})/2$$

where the subscript n denotes the last grid point, and the subscript b the value at the exact end of the glacier: the density of the ice has been divided through the above equation. It follows that the new end point distance is

$$b^{t+\Delta t} = b^t (2\bar{a}_b \Delta t + Z_n^t) + \Delta t V_n (Z_n^t + Z_n^{t+\Delta t}) \tag{4.13}$$

The choice of a triangular snout is somewhat arbitrary, but in the absence of a more reliable shape it is probably the simplest choice. It certainly is easy to use computationally, and more complex snout shapes – such as parabolic, or rectangular – would complicate equation (4.13). The accumulation used in (4.13) is found by direct extrapolation from the last grid point:

$$\bar{a}_b = \bar{a}_n + b\left(\frac{\partial \bar{a}}{\partial x}\right)_n$$

The analysis above holds as long as $0 < b < \Delta x$. Should the left inequality be invalid, then the glacier is shrinking in extent, and if the other inequality is not met, then growth past one grid point has occurred. In both cases the total number of points in the glacier must be adjusted, and a new b computed. This is done quite simply by noting the value of the ice depth at the new last grid point and extrapolating to b using both the triangular snout assumption and the gradient of depth at the last grid point.

The finite difference schemes used for space derivatives are centred ones, but at the extremities of the glacier they must of necessity be replaced by forward or backward analogues. These alternative approximations introduce slight perturbations into the gradient and second derivative patterns and, as it were, provide small 'shocks' at the

boundaries. These effects generally are not apparent some three or more grid spaces away from the source or snout, and even then are evinced only in such very sensitive parameters as the base stress, or the longitudinal strain rate term – the third in equation (4.1).

4.6 Use of the programmes

Equations (4.1) and (4.7) require known distributions of accumulation, bedrock elevation, initial ice thickness, and shape factors before they can be used. These may be supplied in one of three forms: (i) arbitrary values which are read off input cards (such data could also be the results of previous computations), (ii) mathematically specified functions of distance, or (iii) read off magnetic tape (which is the most usual mode for previous results). Consequently any real glacier may be modelled using observational values (input (i)), or idealized by smooth, known analytical functions (input (ii)).

Typical functions which have been used for the modelling of an idealized glacier analogous to the Fedchenko are: quadratic equations giving the bedrock profile and the initial thickness, linear functions of distance for the accumulation, and a constant value for the shape factor. For the results given in section 5, the initial depth profile was a small ice depth (10 cm) everywhere except at the first 10 points where the depth was related to the inverse of the bedrock function so that the elevation slope was a constant. The accumulation then 'created' the glacier. The computation of the 'equilibrium' glacier shape was very lengthy in time, and required many uses of the programme: at each time, the old results were read off the magnetic tape on which they had been stored.

Output of the programme is in three forms also: (i) as printed numbers giving the variables as functions of distance along the grid, (ii) as graphical drawings giving the same distribution schematically – (see curves of Fig. 9 for examples redrawn from such graphs) and (iii) other forms, such as punched cards, magnetic tape. Printing is very quick, but suffers from the disadvantage that the data must be plotted by hand if they are to be easily assimilated, whilst the graphs are easy to work with, but are inordinately wasteful of computer time: a typical graph such as Fig. 9 requires about 10 minutes. Output is generally preset by the programme user, say every 50 time steps, and the most common form is printed matter.

Various man/machine interactions are allowed for by the programme whereby the user can modify the computations as they are performed. Smoothing can be effected at any time; graphs may be called for and drawn at arbitrary times as also can direct printouts; and possibly most important of all, the entire glacier, at any time, can be rescaled so as to lie within a new total number of grid points. Thus if the growth of the glacier was so rapid that a very large number of points was being used, the rescaling would reset the grid space so that the original number of points was restored. Such an option is very necessary since it is not always feasible to use a large grid space initially, and if the number of points grows too big, then the computation time is increased enormously due to the fact that for larger n the iterative solution of velocities requires longer and longer times. It is not feasible, however, to use this rescaling option at all times during the programme so that a constant number of points is employed with a varying grid spacing, thereby obviating the need for computation of the parameter b. This is because problems associated with finite differences and velocities (either block motion or zero) at the snout result in unrealistic rates of growth. This may be explained by the 'shock' that rescaling imposes on the system – a shock which gives large errors in base stress, velocity and hence change in ice thickness near the end of the glacier.

5. RESULTS OF CALCULATIONS FOR THE (TWO-DIMENSIONAL) MODEL

5.1 Approach to steady state

To begin with a large glacier was chosen, similar in size to some of the larger surging glaciers in Alaska. However, since little data were available on some of these glaciers, the data from the Fedchenko Glacier excluding the tributaries was used as a guide.

Since at this stage we are concerned with general features, the data were smoothed so that bedrock and accumulation/ablation profiles were approximated by smooth curves. They are shown in Fig. 7. The initial glacier was negligibly thin at 10 cm

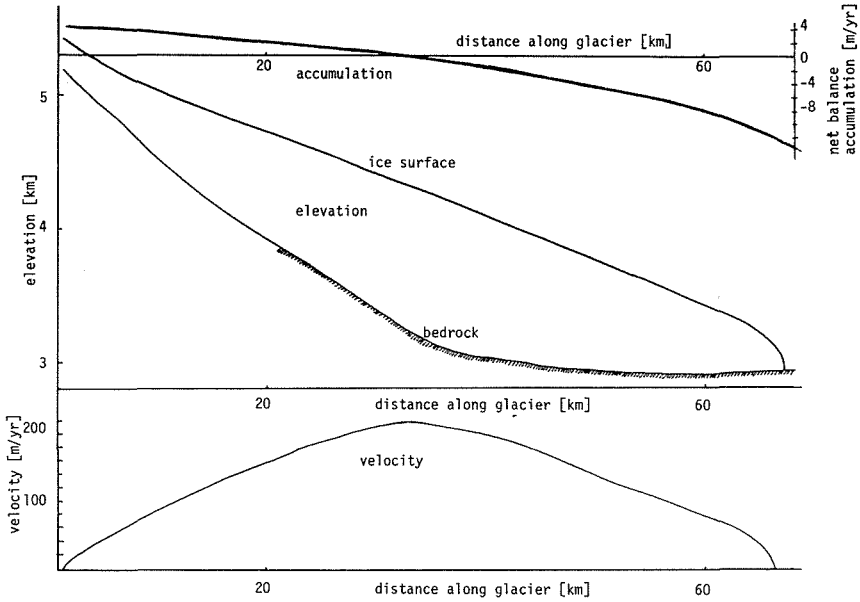

FIGURE 7. Physical parameters of the Fedchenko Glacier.

everywhere except near the snout where the depth reached some metres. (A zero depth initially causes some computational problems.) Under the accumulation/ablation pattern, the glacier shrank to, and past, the firn line within a very short time, then, with the accretion of mass in the higher elevations, slowly grew. This process is presented schematically in Fig. 8.

The upper left pair of curves (solid and dashed) show the rate of growth of both the glacier's total length and thickness at the firn line where these are expressed as fractions of their equilibrium values. The rapid shrinking of the glacier at the onset of the computation is on such a small time scale as not to be noticeable here. The approach to equilibrium (that is to values at a future time infinitely distant) clearly becomes slower and slower as time increases, and this rate of decrease itself slows down. If the deviations between the equilibrium values and those at some particular time (normalized with respect to the equilibrium values) are plotted, the pair of curves on the right results. The deceleration towards equilibrium is also borne out here. From the shape of the two sets of curves it appears that a relation of the form $X = A + B \exp(Ct)$ (where X is either the glacier length or thickness at the firn line and A, B and C are constants, with t being time) might be valid. Further examination of the results, however, shows that there is no value for A which is valid over the entire range of times.

Physically, these results suggest that given an equilibrium glacier – that is, one whose velocity, thickness, bedrock elevation and accumulation are all unchanging with

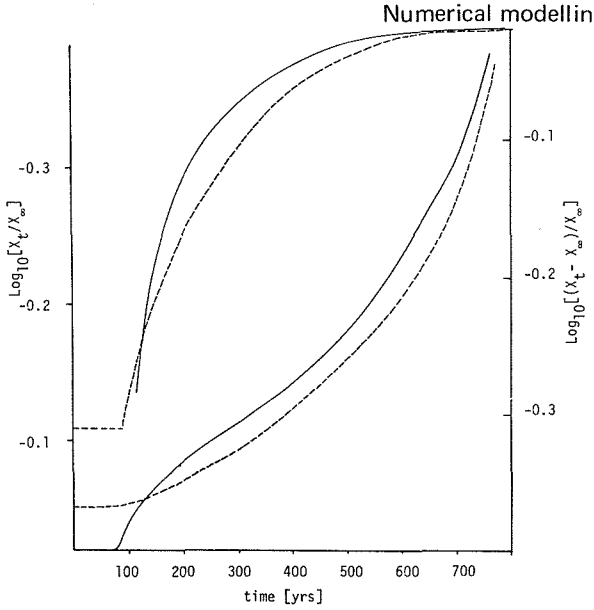

FIGURE 8. Rate of approach of growing glacier to equilibrium. X is either the length of the glacier (dashed curves) or the thickness at the firn line (full curves); X_t is the value at time t; $X\infty$ is value at time ∞ (equilibrium).

time – any deviation from steady-state thicknesses or velocities should result in a return to equilibrium, and this return will be quicker the larger the initial perturbation.

Thus, provided the perturbation does not change the total mass of the glacier too drastically, the equilibrium state should also be a stable one.

Other features of the approach to the equilibrium stage for the growing glacier are given in Fig. 9. The top set of curves shows the elevation profile for the glacier at selected times, the middle set gives the actual thickness and velocity profiles along the glacier, whilst the lowest set indicates the base stress distribution together with the

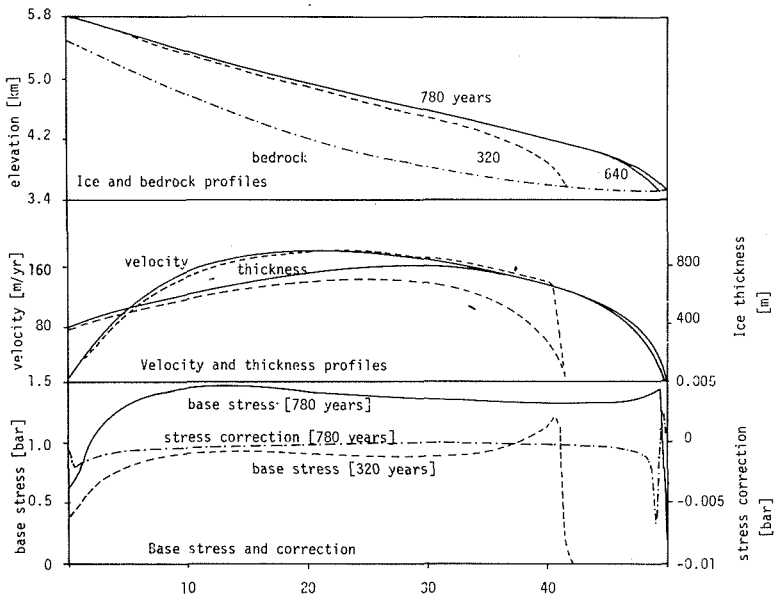

FIGURE 9. Approach to equilibrium. In middle figure, the dashed curves are for 320 years, full curves are for 780 years.

'correction' for the longitudinal stress rate

$$\left(2\tau_0 \frac{\partial}{\partial x}\left\{Z \sinh^{-1}\left[\frac{1}{E_0}\frac{\partial V}{\partial x}\right]\right\}\right)$$

of equation (3.28). The equilibrium profiles are those for 780 years, of course.

The ice thickness and velocity increase to maxima of about 700 m and 150 m/yr respectively and then decrease similarly to zero at the terminus. The base stress is fairly uniform about 1.4 bars along the glacier but is slightly below the average in the compression zone and above in the accumulation zone. The longitudinal stress gradient or correction term is very small except right at the ends where the base stress drops quickly to zero.

5.2 Perturbations from steady state

Several perturbations from the steady state have been studied by simply adding perturbations of three main types to the ice thickness or surface elevation e.g. (i) a uniform slab or (ii) a smooth hump over the upper 10 km of the accumulation zone, and (iii) sinusoidal variations along the surface of differing wavelengths and amplitudes.

The slab and the hump may be considered to consist of an integral over a wide band of wavelengths. The high frequency components die out most rapidly and the long wave components persist for a considerable time (see Fig. 12) causing the perturbation to diffuse out over the entire glacier.

Two slabs were studied, one in which the thickness was 100 metres, and the other wherein it was 200 metres, whilst the maximum thickness for the hump was 100 metres. The speed of the perturbation down the glacier is shown in Table 1, in which it can be seen that the initial disturbance has broken into a number of components.

TABLE 1. Speeds of various components of perturbations superimposed on an equilibrium or steady-state glacier. The velocity at 4 years is close to the equilibrium value

	Slab 100	Slab 200	Hump
Maximum initial velocity	1901 m/yr	9000 m/yr	522 m/yr
Maximum velocity at 4 years	236	316	212
Speed of the 'crest' of the velocity wave	1250	1375	1250
Speed of the 'crest' of the thickness change with time	2500	3375	2125

The velocity maximum associated with the disturbance moves down the glacier at a very high speed: this 'crest' in the velocity distribution has a motion about 4 to 5 times faster than the maximum velocity. At each point of the ice the thickness is changing with time due to the perturbation. This rate of change gives rise to another wave moving down the glacier. As can be seen from the above table the speed for the crest of this wave moves at about an order of magnitude faster than the most rapidly moving ice in the glacier.

The wave of the thickness change with time moves both up and down the glacier away from the initial point of maximum disturbance. From the results it seems as though there is little or no reflection of the trough which moves to the source once it reaches that point. The trough merely remains more or less stationary and fills in with time.

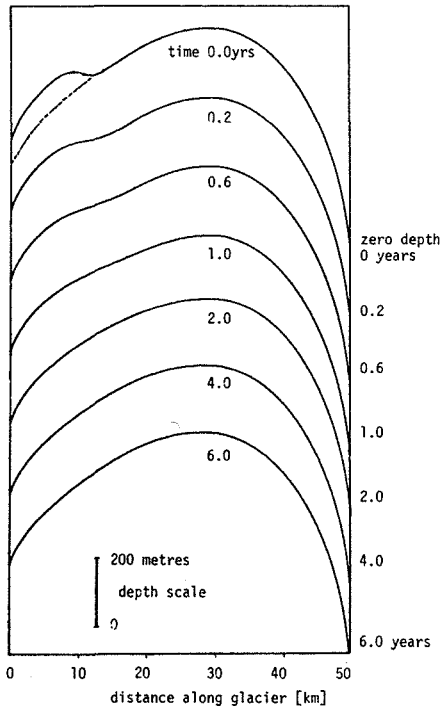

FIGURE 10a. Glacier thickness after impressed perturbation of slab at source. Slab thickness, 100 m.

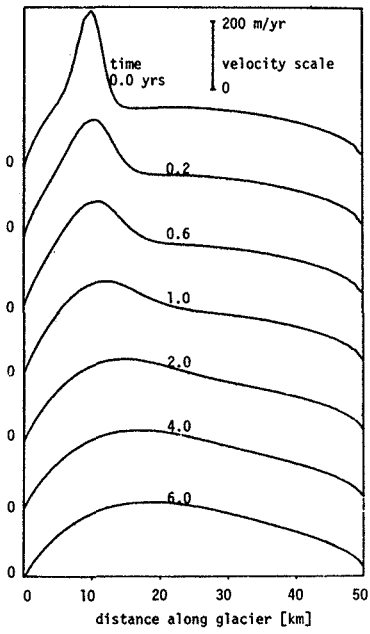

FIGURE 10b. Glacier velocities after impressed perturbation of slab at source. Slab thickness, 100 m.

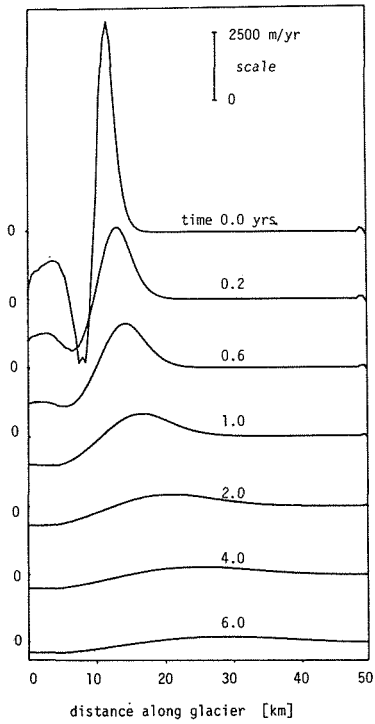

FIGURE 10c. Glacier rate-of-change-of-thickness after impressed perturbation of slab at source. Slab thickness, 100 m.

By the time the velocity and thickness change waves reach the snout of the glacier their amplitude is very small indeed – at least for the cases studied – and no surging takes place. The glacier does move forward somewhat under the influence of the increased mass, added by the perturbation, but takes up a new equilibrium shape and velocity profile almost indistinguishable from the old.

The speeds of the two crests of Table 1 are reasonably constant with time and it appears from the limited data that their magnitude is related most directly to the amount of ice initially added to the equilibrium glacier. It might be thought from this that simply increasing the amplitude of the initial disturbance might result in a surge. However, even apart from the questionable physical validity of such a procedure, the excessively large gradients set up within the ice of such parameters as thickness, surface elevation, velocity and base stress cannot be adequately handled by the model and either computational instability results or the iterative solution for velocities refuses to converge.

Further information is given in Fig. 10 for the case of the slab of 100 m thickness. The first set of curves gives the depth profile at various times, the second set shows the velocity profile, and the third set gives the rate of change of thickness with time. It is clear from all curves how quickly the glacier approaches the equilibrium state even for such a gross disturbance. Also quite apparent for the first few graphs are the crests of the waves of Table 1; to find these features at times greater than one year, the detailed printout of the computer must be consulted. Similar graphs hold for the other disturbances.

The rate of approach to the new equilibrium state for each of these three cases is shown in Fig. 11. The smooth nature of the curves of Fig. 8 has become modified here, particularly for the thick slab. It is difficult to account for the fluctuations of

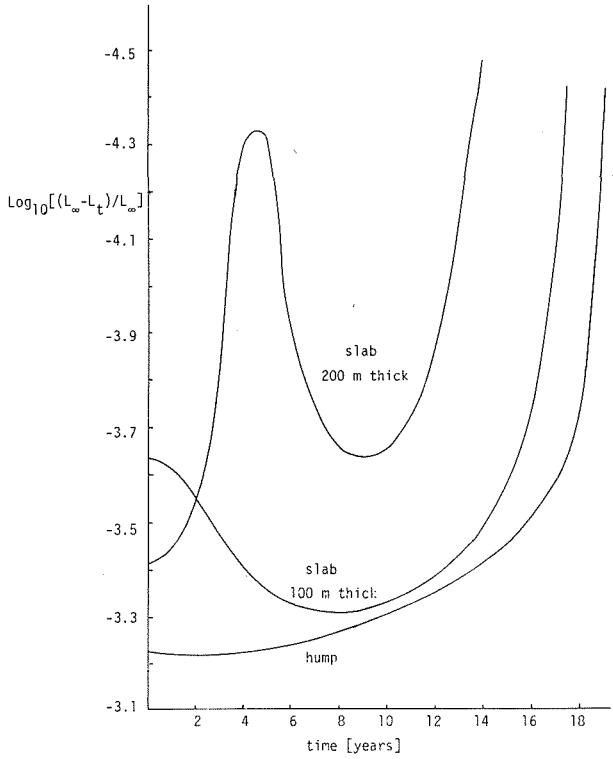

FIGURE 11. Rate of approach to equilibrium for slab and hump perturbations.

that curve, and it is probably a reflection of the severe test that that disturbance makes on the model. For the thinner slab, the initial dip in the curve (indicating a shrinkage of the glacier) can be accounted for by the velocities: the new thickness profile produces a new velocity profile such that the velocity gradient decreases near the snout. This in turn means that mass transport to the glacier end is reduced, and ablation will shrink the ice mass. After a while, the velocity wave diffuses down the glacier and it grows again. For the 200 m slab, it is thought that the changes wrought in the velocity profile by the discontinuity in thickness at the edge of the superposed slab have much more complex effects on the growth or shrinkage of the glacier snout initially.

The third kind of perturbation employed was sinusoidal disturbances, of various amplitudes and wavelengths, such that an integral number of waves fitted along the glacier. This meant that regardless of the phase of the disturbance, the total mass of the glacier was undisturbed. The new equilibrium parameters and profiles should be exactly the same as the old. This in fact was always observed. Some of the results obtained with these perturbations are shown in Fig. 12.

The four sets of curves correspond to two amplitudes and two wavelengths of disturbance: amplitudes of 25 and 12.5 m, and wavelengths of 10 and 50 grid points (or 5 and 25 km), respectively. The parameter of the disturbance depicted in the figure is the rate of change of thickness with time. This was chosen since it is the most sensitive feature of the perturbation, and a new equilibrium is clearly shown by a flat trace. It can be seen from the curves for the 50 point wavelengths that an increased amplitude results in a longer time to reach equilibrium again – in accordance with the results discussed previously. Although it is not so well defined for the shorter wavelengths, a similar result is seen for them. Again, in spite of the very much larger

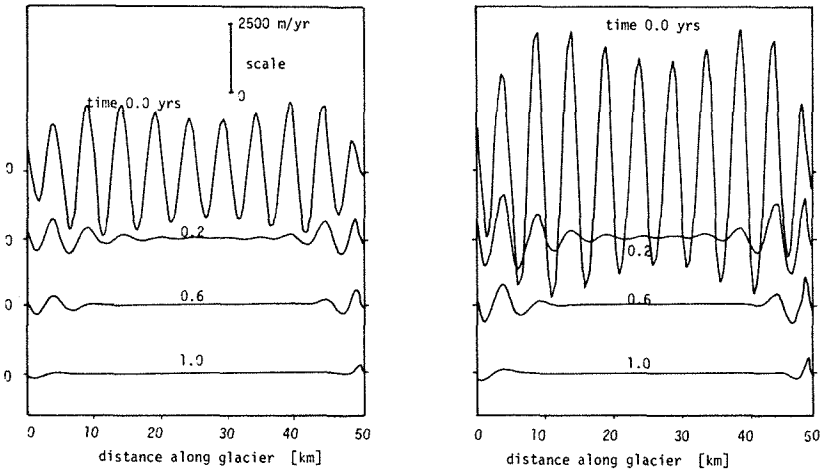

FIGURE 12a. Approach to equilibrium for impressed sinusoidal perturbation. Left figure is for amplitude of 12.5 m, right figure is for amplitude of 25 m. Wavelength in both cases is 10 grid units (5 km).

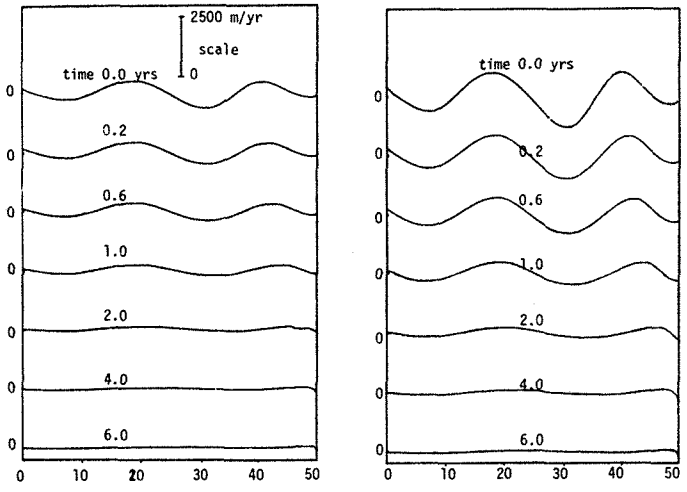

FIGURE 12b. Approach to equilibrium for impressed sinusoidal disturbance. Left figure is for amplitude 12.5 m, right is for 25 m. For both, the wavelength is 50 grid units (25 km).

amplitude of the initial disturbance, the shorter wavelength is damped out much more quickly than the longer, and only some residual effects at the source and snout of the glacier are observed after one year. (The larger initial amplitude in the thickness change is due to the greater changes in the surface slope imposed by the shorter wavelength disturbance.) Of great interest is the evidence in the shorter wavelength curves at time zero of a larger perturbation, of some 5 times greater wavelength. This is manifest in the wave-like character of the maxima and minima of that curve. Computationally, it is thought that this is due to an 'aliasing' effect of the finite difference schemes used, or to the smoothing operator employed (which uses 5 grid points). However, the wavelength of only 10 grid points is rather small, and it appears that the aliasing may have a physical explanation since the shorter wavelength perturbations strictly require the addition of the variational term in the stress equations. These have not yet been well studied.

The rate of approach to steady state of the sinusoidal perturbations is given in Fig. 13. Here, the ordinate is the ratio of the amplitude of the disturbance at any time to its initial value, and is plotted logarithmically. The curves may be grouped into four pairs, corresponding to four different wavelengths: 100, 50, 25 and 10 grid units, where 100 grid units is equivalent to the total glacier length. The amplitude of the initial disturbance is the same for all curves – 25 m – but the phase of the disturbance is 180° apart for each member of each pair. Thus, for example, for the 100 grid wavelengths, the curve marked + corresponds to addition of mass for the first half of the glacier and subtraction for the latter half, whilst the curve labelled – denotes subtraction of mass for the first half, and then addition thereafter. In all but the 10 wavelength case, the addition of mass near the source, rather than the removal, results in a more rapid approach to equilibrium. However, addition at the source means removal at the snout, and it appears from the figure, therefore, that the approach to equilibrium is more rapid when the glacier grows up to the steady-state shape, rather than when it shrinks down to it. Further examination of this aspect of the results should indicate whether it is a purely computational or physical phenomenon.

The result for the 10 grid wavelength disturbance is somewhat of an anomaly, but appears related to computational techniques, and in particular to the aliasing phenomenon mentioned in the discussion of Fig. 12. It would seem that boundary

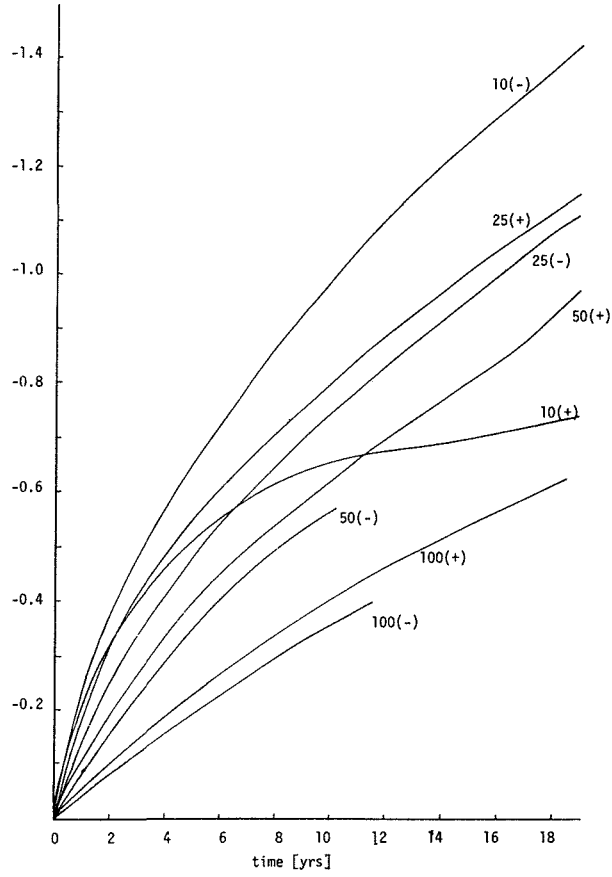

FIGURE 13. Approach to equilibrium for impressed perturbation of sinusoidal nature. Numbers on curves indicate wavelength of perturbation in grid units (1 unit = 0.5 km), and (+) indicates addition of mass at source, (–) indicates subtraction of mass at source.

problems at the snout are also of importance for it is otherwise difficult to explain the difference between the rate of approach to equilibrium for the growing and shrinking glaciers. Results, not shown here, for a wavelength of 5 grid units exhibit the same anomalous behaviour.

It is apparent from this figure that the larger wavelengths have a much slower approach to equilibrium, and that the phase of the disturbance is a second-order effect. All of these sinusoidal perturbations exhibit stationary behaviour: thus, for example, the velocity profile, in contrast to that for the slabs or hump, has its extrema always in the same location.

Other perturbations that have been studied include a large ice mass well above steady state in the accumulation zone and a reduced remnant in the ablation zone. In this case the ice did move down at 'normal advance' not 'surge' speed and went beyond the steady-state terminus but only in the process of levelling out and for ever gradually approached the steady state.

In all cases considered the steady-state position was found to be stable to perturbations. This appears to be the nature of the equilibrium equations with essentially single valued boundary conditions which thus give rise to a unique steady-state solution. In order to generate oscillating or periodic states (with accumulation constant) it is necessary to study double valued boundary conditions. However, because of space limitations, the sliding and surging models will be given elsewhere.

6. A THREE-DIMENSIONAL MODEL

Much remains to be done with the simple one-dimensional model described here, but two fundamental drawbacks inherent in it should be pointed out, and indications given as to how these deficiencies may be removed. First, the model provides only a cross-section of any glacier, even though transverse changes in bedrock elevation and ice thickness may be parameterized through the shape factor. Second, no attempt has been made to adjust the dynamics of the ice mass for changes in temperature during the flow. This reciprocal feedback process where velocity changes temperature through friction and then temperature modifies the velocity through the flow law is extremely important, but unfortunately difficult to model. The nature of the feedback will clearly amplify exponentially any errors in the initial data, or, which is practically equivalent, any deficiencies in the flow law used. Nonetheless, a start has been made on such modelling, and preliminary results already obtained.

The new model which will be outlined very briefly here is applicable to any sized ice mass of any arbitrary shape, and the calculations so far have been performed for the Greenland ice sheet. This was selected since a parallel set of calculations on temperatures and dynamics using one-dimensional models was already under way and would provide useful checks on the new model.

The basic equations used are those of continuity of mass, and the heat conduction equation in three dimensions. Two continuity equations are employed, one for the ice in a vertical of the coordinate system, and one for any particular element. Details of these will be given elsewhere. Boundary problems associated with a fixed grid can become acute: for example, as the ice grows either vertically or horizontally it moves past the mesh points, and as with the glacier model described earlier in this paper, 'shocks' arise due to the sudden addition of new mass (or points). To overcome such problems a coordinate system is set up such that the horizontal axes parallel the ice surface and base at all points, and the vertical coordinate always has the value zero at the surface and unity at the base of the ice. (Details of this set of axes for a simple one-dimensional model may be found in Budd, Jenssen and Radok, 1971). With the transformation of axes, terms such as $\nabla^2 T$ and ∇T in the basic equations are also modified and in fact become much more complex. The level of complexity and the

concomitant increase in computation time, however, do not produce nearly as many difficulties as trying to cope with a truly Eulerian system and sudden shocks.

Ancillary equations in the model govern the rate at which heat is input to the ice at any particular point, phase changes, amounts of melt and so forth. The velocity distribution is determined at any point through a flow law which is specified in tabular form and is based on considerations discussed in section 2.3. Frictional heating can take either of two forms – one in which it is a function of the strain rate and is spread throughout the vertical, and one in which it is concentrated at the base of the ice column. If the heating is great enough, or if the ice begins to move into the ocean, then phase changes (melting and freezing) can occur. These are noted by the model and adjustments made to the thickness accordingly.

The main sequence of operations in the computer use of the model is to determine the velocity distribution in three dimensions from the existing temperatures, to use the equations of continuity and those governing phase changes to obtain a new depth distribution, and then to repeat this cycle. Problems can arise in connection with the computational stability of the integration procedure, and these necessitate the use of a time step which is a function of the ice depth, accumulation and velocity, and therefore changes from point to point of the grid.

7. FUTURE WORK

Although the present glacier model is useful for many applications to glacier growth, decay and climatic change, a great deal still remains to be done to achieve a programme which can cover all possibilities of glacier motion.

One generalization at present underway, and discussed in section 6, is the development of a new three-dimensional model which incorporates temperature effects through the heat conduction equation coupled with the dynamics. Any three-dimensional grid requires a great deal of computer storage so at present this programme is being developed for a very coarse spacing model of the Greenland ice sheet as a trial.

Complex effects on the flow such as temperature, water content, ice fabrics, etc., can all be incorporated into a general model once it is possible to relate them to the stress, strain rate, or history through the trajectories and particle paths.

Even with the existing models it is possible to carry out a large number of investigating calculations to provide insight into the fields of travelling waves in glaciers and glacier surges. However, at this stage in order to evaluate such calculations we need the results of more field measurements of these phenomena. By working backwards from the field results it should prove possible to derive the approximate bulk parameters for flow and basal friction or stress that govern the flow.

Acknowledgements. The authors wish to indicate their indebtedness and gratitude to J. Jacka, Susan Moir and Vonne Murphy for their aid in data reduction and preparation of the manuscript, and to Drs G. de Q. Robin and U.Radok whose stimulation and insight were invaluable.

REFERENCES

Bauer, A. (1968) Missions aériennes de reconnaissance au Groënland 1957-58. *Meddelelser om Grønland,* Bd. 173, Nr. 3, 116 pp.

Bowden, F. P. and Tabor, D. (1967) *Friction and lubrication.* Methuen, London.

Budd, W. F. (1969) The dynamics of ice masses. ANARE Scientific Reports, Publ. No. 108. 212 pp.

Budd, W. F. (1970a) The longitudinal stress and strain rate gradients in ice masses. *J. Glaciol.,* 9 (55), 19-27.

Budd, W. F. (1970b) Ice flow over bedrock perturbations. *J. Glaciol.,* 9 (55), 29-48.

Budd, W. F. (1971) Stress variations with ice flow over undulations. *J. Glaciol.*, **10** (59).
Budd, W. F. *et al.* (1971) *Derived physical characteristics of the Antarctic Ice Sheet,* by W. F. Budd, D. Jenssen and U. Radok, University of Melbourne, Department of Meteorology, Publ. No. 18.
Campbell, W. J. and Rasmussen, L. A. (1969) Three dimensional surges and recoveries in a numerical glacier model. *Can. J. Earth Sciences,* **6** (4) Pt. 2, 979-86.
Campbell, W. J. and Rasmussen, L. A. (1970) A heuristic numerical model for three dimensional time dependent glacier flow. ISAGE Symposium, SCAR, Commission of Snow and Ice, IASH Publ. No. 86, 177-90.
Carbonnell, M. and Bauer, A. (1968) Exploitation des couvertues photographiques aériennes répétées du font des glaciers mêlant dans Disko Bugt et Umanak Fjord, juin-juillet 1964. *Meddelelser om Grønland,* Bd. 173, Nr. 5, 78 pp.
Glen, J. W. (1955) The creep of polycrystalline ice. *Proc. Roy. Soc.*, Ser. A, **228**, 519-38.
Glen, J. W. (1958) The flow law of ice. Symposium of Chamonix. IUGG IASH Publ. No. 47.
Jenssen, D. and Straede, J. (1969) The accuracy of finite difference analogues of simple differential operators. *Proceedings WMO/IUGG Symposium on Numerical Weather Prediction, Tokyo.* Japan Meteorological Agency, Tokyo, pp. vii-59–vii-76.
Kamb, B. (1970) Sliding motion of glaciers: theory and observation. *Reviews of Geophysics and Space Physics,* 8 (4), 673-728.
Kamb, W. B. and Shreve, R. L. (1966) Results of a new method for measuring internal deformation in glaciers. *Trans. Amer. Geophys. Union,* **47** (1), 190.
Lliboutry, L. (1965) *Traité de glaciologie.* Paris, Masson et Cie.
Lliboutry, L. (1968a) Théorie complète du glissement des glaciers, compte tenu du gluage transitoire. Assembly of Berne. IUGG IASH Publ. No. 79, 33-48.
Lliboutry, L. (1968b) General theory of subglacial cultivation and sliding of temperate glaciers. *J. Glaciol.*, 7 (49), 21-58.
Lliboutry, L. (1969) Contribution à la théorie des ondes glaciaires. *Can. J. Earth Sciences,* 6 (4) Pt. 2, 943-53.
Lliboutry, L. (1971) Permeability, brine content and temperature of temperate ice. *J. Glaciol.*, **10** (58), 15-30.
Meier, M. F. (1960) Mode of flow of Saskatchewan Glacier, Alberta, Canada. US Geological Survey Professional Paper 351, 70 pp.
Nye, J. F. (1953) The flow law of ice from measurements in glacier tunnels, laboratory measurements and the Jungfraufirn borehole experiment. *Proc. Roy. Soc.*, Ser. A, **219**, 447-89.
Nye, J. F. (1960) The response of glaciers and ice sheets to seasonal and climatic changes. *Proc. Roy. Soc.*, Ser. A, **256**, 559-84.
Nye, J. F. (1963a) On the theory of the advance and retreat of glaciers. *Geophys. J. of the Royal Astronomical Society,* 7 (4), 431-56.
Nye, J. F. (1963b) The response of a glacier to changes in the rate of nourishment and wastage. *Proc. Roy. Soc.*, Ser. A, **275** (1360), 87-112.
Nye, J. F. (1965a) The frequency response of glaciers. *J. Glaciol.*, 5 (41), 567-87.
Nye, J. F. (1965b) A numerical method of inferring the budget history of a glacier from its advance and retreat. *J. Glaciol.*, 5 (41), 589-607.
Nye, J. F. (1965c) Theory of glacier variations; reply to Dr Shumskiy's letter. *J. Glaciol.*, 5 (45), 465 [letter].
Nye, J. F. (1965d) The flow of a glacier in a channel of rectangular, elliptic or parabolic cross section. *J. Glaciol.*, 5 (41), 661-90.
Nye, J. F. (1966) Theory of glacier variations; reply to Dr Shumskiy's letter. *J. Glaciol.*, 6 (45), 456.
Nye, J. F. (1969) A calculation on the sliding of ice over a wavy surface using a Newtonian viscous approximation. *Proc. Roy. Soc.*, Ser. A, **311**, 445-67.
Nye, J. F. (1970) Glacier sliding without cavitation in a linear viscous approximation. *Proc. Roy. Soc.*, Ser. A, **315**, 381-403.
Paterson, W. S. B. and Savage, J. L. (1963) Measurements on Athabasca Glacier relating to the flow law of ice. *J. Geophys. Res.*, **68**, 4537-43.
Shreve, R. L. and Sharp, R. P. (1970) Internal deformation and thermal anomalies in lower Blue Glacier, Mt. Olympus, Washington, USA. *J. Glaciol.*, 9 (55), 65-86.
Shumskiy, P. A. (1964) *Principles of structural glaciology.* Dover, 497 pp.
Shumskiy, P. A. (1965) Theory of glacier variations. *J. Glaciol.*, 5 (40), 515-17.
Shumskiy, P. A. (1966) Theory of glacier variations; reply to Dr. Nye's letter. *J. Glaciol.*, 6 (45), 465.
Tabor, D. and Walker, J. C. F. (1970) Creep and friction of ice. *Nature,* **228**, 137-9.
Untersteiner, N. and Nye, J. F. (1968) Computations of the possible future behaviour of Berendon Glacier, Canada. *J. Glaciol.*, 7 (50), 205-13.
Weertman, J. (1957) On the sliding of glaciers. *J. Glaciol.*, **5**, 33-8.

Weertman, J. (1962) Catastrophic glacier advances. Symposium of Obergurgl. IUGG IASH Publ. No. 58.

Weertman, J. (1964) The theory of glacier sliding. *J. Glaciol.*, **5**, 287-303.

Weertman, J. (1967) An examination of the Lliboutry theory of glacier sliding. *J. Glaciol.*, **6**, 489-94.

Weertman, J. (1969) Water lubrication mechanism of glacier surges. *Can. J. Earth Sciences*, **6** (4) Pt. 2, 920-42.